TOWARD A RAYLEIGH WAVE ATTENUATION MODEL FOR CENTRAL ASIA

Anatoli L. Levshin[1], Xiaoning (David) Yang[2], Michael H. Ritzwoller[1], Mikhail P. Barmin[1], and Anthony R. Lowry[1]

University of Colorado at Boulder[1] and Los Alamos National Laboratory[2]

Sponsored by National Nuclear Security Administration
Office of Nonproliferation Research and Development
Office of Defense Nuclear Nonproliferation

Contracts Nos. DE-FC52-05NA26608[1] and W-7405-ENG-36[2]

ABSTRACT

We report on progress toward an attenuation model for short-period (10-25 s) Rayleigh waves in Central Asia. This model will be defined by maps of attenuation across the region of study in the specified period band. The model is designed to calibrate the regional surface wave magnitude scale and to extend the teleseismic M_S-m_b event discriminant to regional distances. In order to apply the M_S-m_b discriminant to regional-distance monitoring, a modified M_S formula using shorter-period (< 20) surface wave amplitudes is required (e.g., Marshall and Basham, 1972; Bonner et al., 2006; Russell, 2006). Work is progressing in three stages: (1) data accumulation and amplitude measurement, (2) estimation of attenuation coefficients, and (3) tomography. To date, efforts have been devoted primarily to the first stage.

The first stage in the model construction is the measurement of Rayleigh-wave spectral amplitudes. Inherent difficulties result from multipathing and scattering of short-period surface waves crossing strong lateral inhomogeneities in the crust. To overcome these difficulties, we apply the Surface Wave Amplitude Measurement Tool (SWAMTOOL) designed at Los Alamos National Laboratory (LANL), which incorporates dispersion analysis, phase-matched filtering, and additional means to estimate the quality and reliability of the measurements. We have enhanced SWAMTOOL by providing improved options for phase-matched filtering of the surface wave signals. The similarity of the results now obtained with SWAMTOOL and the Frequency-Time Analysis (FTAN) algorithm designed at CU-Boulder, as well as numerous repeatability tests, confirm the validity of the measurements. We currently are collecting and processing both two-station and single-station waveform data. The existing broadband station distribution and the pattern of seismicity provide a sufficient number of spectral amplitude measurements between 12 and 20 s for the construction of the 2-D tomographic maps of attenuation coefficients. Measurements at periods below about 12 s are too scarce for tomographic inversion.

In the second stage of the work, spectral attenuation coefficients are estimated using both interstation amplitude measurements and single-station measurements, corrected for the source and receiver terms. Current work focuses on simulated data, which demonstrate the existence of a strong dependence of Rayleigh-wave amplitude spectra on source parameters, particularly the source depth, and the structure of the crust near the source and receiver regions that grows as periods decrease. It is, therefore, necessary to include additional variables related to the source into the inversion of the observed data and also to apply an existing 3-D model of the Eurasian crust in the data inversion. Work is now beginning to transition to this next stage, the estimation of attenuation coefficients from the observations. Particular emphasis is now being placed on accounting for uncertainties in source parameters and variations in the 3-D structure of the Central Asian crust.

OBJECTIVES

The objectives of the study are (1) to develop short-period (10–18 s), two-dimensional (2-D) Rayleigh-wave attenuation models for Central Asia, along with associated uncertainty statistics, through a tomographic approach, and (2) to calibrate Russell's (2006) M_S formula with these models for the same region.

RESEARCH ACCOMPLISHED

Introduction

Knowledge of the losses of seismic energy during the propagation of the wave from the source to receivers is essential for the estimation of the surface wave magnitude M_S and the seismic moment of the source. This is especially important for monitoring underground nuclear explosions, in which the estimation of M_S is used as a part of the most robust seismic discriminant, the M_S-m_b discriminant. In order to apply this discriminant to regional-distance monitoring, a modified M_S formula using shorter-period (< 20) surface wave amplitudes is required (e.g., Marshall and Basham, 1972; Bonner et al., 2006; Russell, 2006). The purpose of this work is to construct short-period (10–18 s) 2-D Rayleigh-wave attenuation models for Central Asia and to use them to calibrate M_S formula of Russell (2006).

We are currently in this study's first stage, in which we have collected and processed broadband records following seismic events within and around Central Asia. To determine the amplitude spectra of the surface waves, we apply the SWAMTOOL (Yang at al., 2004, 2005). Early applications indicated the need to enhance SWAMTOOL by improving the phase-matched filtering of the surface waves. This paper summarizes the resulting improvements, the comparisons of SWAMTOOL measurements with those from FTAN (Levshin et al., 1989; Ritzwoller and Levshin, 1998) and characterizes the observed data set of spectral amplitude measurements.

The next phase of this study will be the estimation of attenuation coefficients from the observed spectral amplitudes using both single-station and interstation measurements. Measurements of the first type must be corrected for the source and receiver terms and the latter for the receiver terms. At this stage of work, we will focus on simulating these effects and evaluating their influence on the observed attenuation coefficients.

Elements of Theory

We assume that surface waves propagate in a laterally and radially inhomogeneous medium, in which elastic and anelastic parameters change smoothly along the Earth's surface. The term "smoothly" means that the changes of these parameters (wave speeds, densities, thicknesses of layers, Q_s along the distance of a wavelength) are small (e.g., Woodhouse, 1974; Levshin et al., 1989). Surface waves are generated by a point source with a moment tensor **M**. The tensor and coordinates of the source, including depth h, are presumed to be known. Then the amplitude spectrum $U(\omega)$ of the surface wave mode recorded by a receiver situated on the Earth's surface at the epicentral distance Δ and in azimuthal direction φ from the epicenter can be presented approximately as

$$U(\omega) = S(\omega, h, \varphi, \mathbf{M}(\omega)) \times P(\Delta, \omega) \times R(\omega) \quad .$$

Here, ω is a frequency in rad/s. The source term S depends also on the Earth's structure near the source. The propagation term P is defined by the elastic and anelastic structure between the source and receiver. Assuming that the wave propagates along the great circle between source and receiver, we have

$$P = \frac{\exp(-\omega \int_L \frac{dl}{2u(\omega,l)Q_s(\omega,l)}}{\sqrt{k(\omega) r_o \sin\Delta}} = \frac{\exp(-\int_L \alpha_s(\omega,l)dl}{\sqrt{k(\omega) r_o \sin\Delta}} \quad ,$$

where r_0 is the Earth's radius, u is group velocity, k is wavenumber, Q_s is the surface wave Q-factor, and α_s is the surface wave attenuation coefficient. The integral $I = \int_L \alpha_s(\omega, l)dl$ is taken along the great circle through the source and receiver. The receiver term R depends on the structure near the receiver and the frequency response of the instrument. In the case when we have two stations at approximately the same azimuth φ from the source, it is possible to use the ratio of two observed spectra $U_1(\omega)$ and $U_2(\omega)$ to find the integral I_{12}

$$I_{12} = \int_{L_{12}} \alpha_s(\omega, l)dl = \ln\left[\frac{U_1 R_2 \sqrt{\sin \Delta_1}}{U_2 R_1 \sqrt{\sin \Delta_2}}\right],$$

where L_{12} is the path between stations and $\Delta_2 > \Delta_1$. Our goal is to find the values of integrals $I(\omega_i)$ and $I_{12}(\omega_i)$ for all appropriate combinations of receivers and stations or pairs of stations for a set of values of frequencies ω_i in the frequency band of study.

Data Collection

We are currently collecting and processing surface wave waveform data. In the first stage of data collection, we processed around 100 events that occurred in and around Eurasia in 2003–2005. Several global and regional broadband networks have existed in Eurasia during the considered time interval. These include Global Seismographic Network (GSN), International Monitoring System (IMS), GEOSCOPE, GEOFON, Mediterranean Seismic Network (MEDNET), China Seismological Digital Network (CDSN), Kyrgyz Seismic Network (KNET), Kazakhstan Seismic Network (KAZNET), and others available through the IRIS Data Management Center (IRIS DMC). More than 10,000 broadband records of about 100 stations were selected for processing. The map with the event and station distribution used at this stage of work is shown in Figure 1. Records were converted from the Standard for the Exchange of Earthquake Data (SEED) into the Seismic Analysis Code (SAC) format and transformed into ground displacement.

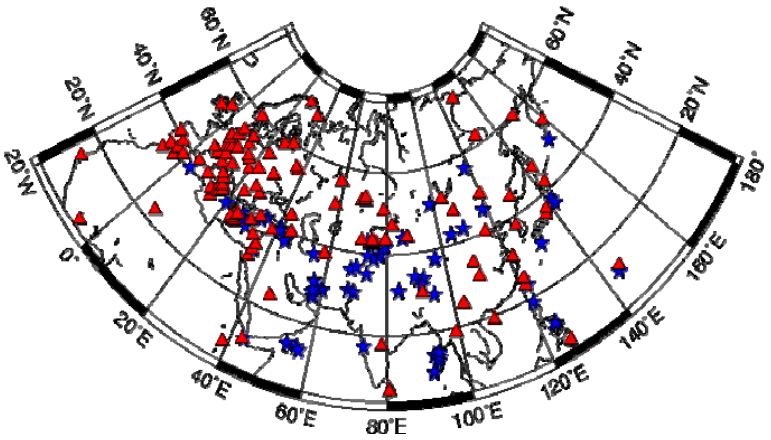

Figure 1. Distribution of epicenters (stars) and stations (triangles) selected for spectral amplitude measurements.

Measurements

The accuracy of surface wave attenuation measurements is affected by uncertainties in source-parameter estimates and site responses and by medium elastic effects, with medium elastic effects such as multipathing, focusing, defocusing, and off-great-circle propagation being among the principal sources of error (Mitchell, 1995; Selby and Woodhouse, 2000). As part of a previous 20 s surface wave attenuation study, LANL researchers designed a SWAMTOOL to address some of these uncertainties (Yang et al., 2004).

We developed several SWAMTOOL improvements, which provide more opportunities for efficient phase-matched filtering of the signal (e.g., Herrin and Goforth, 1977; Russell et al., 1988). A snapshot of SWAMTOOL data processing for an event in Tibet on 04/10/2004 with Ms = 5.1, recorded by the station KMI, is shown in Figure 2. The first step in the analysis of a selected signal (upper right window) is transforming it into the frequency-time domain (upper left window) and tracing the maximum amplitude as a function of frequency ("raw" group velocity curve). Depending on the pattern on the diagram, an analyst makes a decision about the presence and frequency range of the desired signal, i.e., the fundamental mode of the Rayleigh wave. The analyst may either (1) reject the record, (2) construct a phase-matched filter based on prediction from a recently developed surface-wave group velocity model (e.g., Ritzwoller and Levshin, 1998; Levshin and Ritzwoller, 2003; Stevens et al., 2001; Levshin et al., 2003), (3) construct a phase-matched filter using the raw group velocity curve in a chosen frequency range, or (4) construct a phase-matched filter using the curve he/she draws across the diagram.

The filtered signal is then windowed in the time domain to suppress noise and is used for measuring the amplitude spectrum (lower left window). This filtering process and other aspects of the measurement tool (lower right window), such as the analysis of the theoretical source spectrum and radiation pattern and the comparison of observed and geometrical back-azimuths, are designed to reduce the bias caused by multipathing and focusing/defocusing.

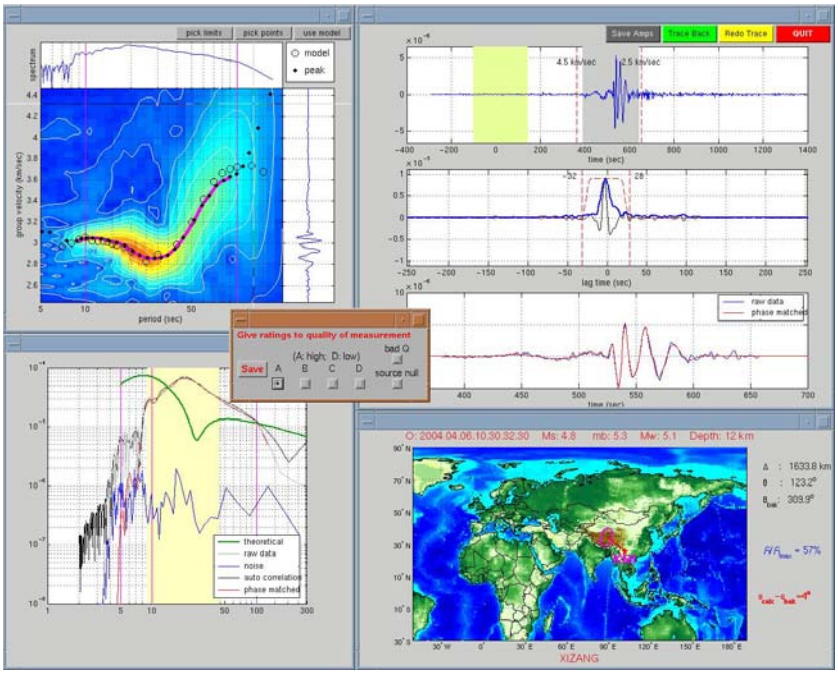

Figure 2. Snapshot of SWAMTOOL for an event in Tibet recorded by station KMI.

The similarity of the results now obtained with SWAMTOOL and the FTAN algorithm designed at CU-Boulder, as well as numerous repeatability tests, confirm the validity of the measurements (Figure 3).

Characterization of the Spectral Amplitude Data

More than 6,000 spectral amplitude measurements were obtained using SWAMTOOL interactively. The amount of measurements significantly varies with period. The paths corresponding to the measurements at different periods are shown in Figure 4. Figure 5 shows the number of measured spectral amplitudes as a function of period. The existing broadband station distribution and the pattern of seismicity provide a sufficient number of source/station spectral amplitude measurements in a 12 to 20 s period for the construction of the 2-D tomographic maps of attenuation

coefficients. Measurements at periods below about 12 s are too scarce. Figure 6 characterizes aspects of the observed data set. The M_b magnitudes of the selected events vary from 4 to 7, with dominant magnitudes near 5. The M_s magnitudes are mostly in the 5 to 6 range. Epicentral distances widely vary from 500 to 8000 km with most path lengths between 2000 and 6000 km. Source depths (according to the Preliminary Determination of Epicenters [PDE] catalog) are between 5 and 40 km. Note the significant difference between source depths provided by the Harvard-Centroid-Moment Tensor (CMT) and PDE catalogs (Figure 6d). The peak of the distribution in Figure 6d is caused by different default values in the PDE and CMT catalog when event depth is ill-constrained (10 km for PDE, 15 km for CMT). This indeterminacy of event depths applied a significant side-constraint on the use of amplitude spectra data, as discussed further in this report.

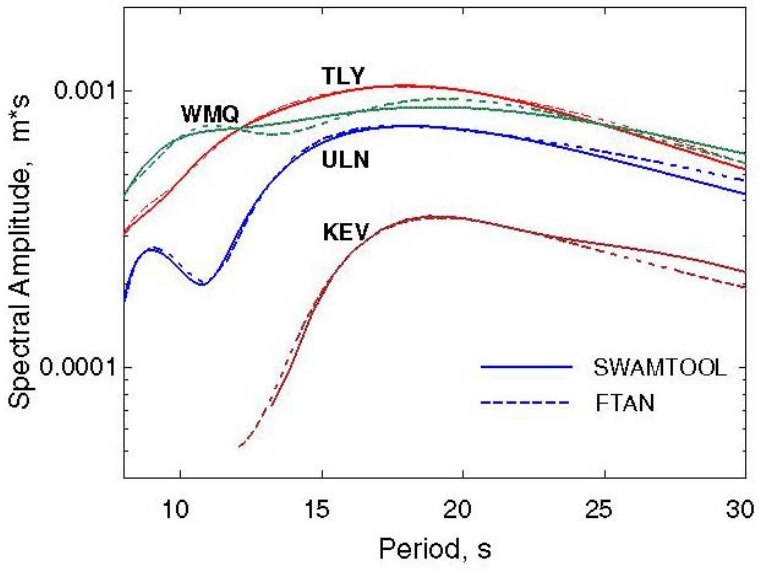

Figure 3. Comparison of the spectral amplitude measurements made with SWAMTOOL and FTAN from an earthquake on 06/01/2005 near the India-China border region (Ms = 5.7).

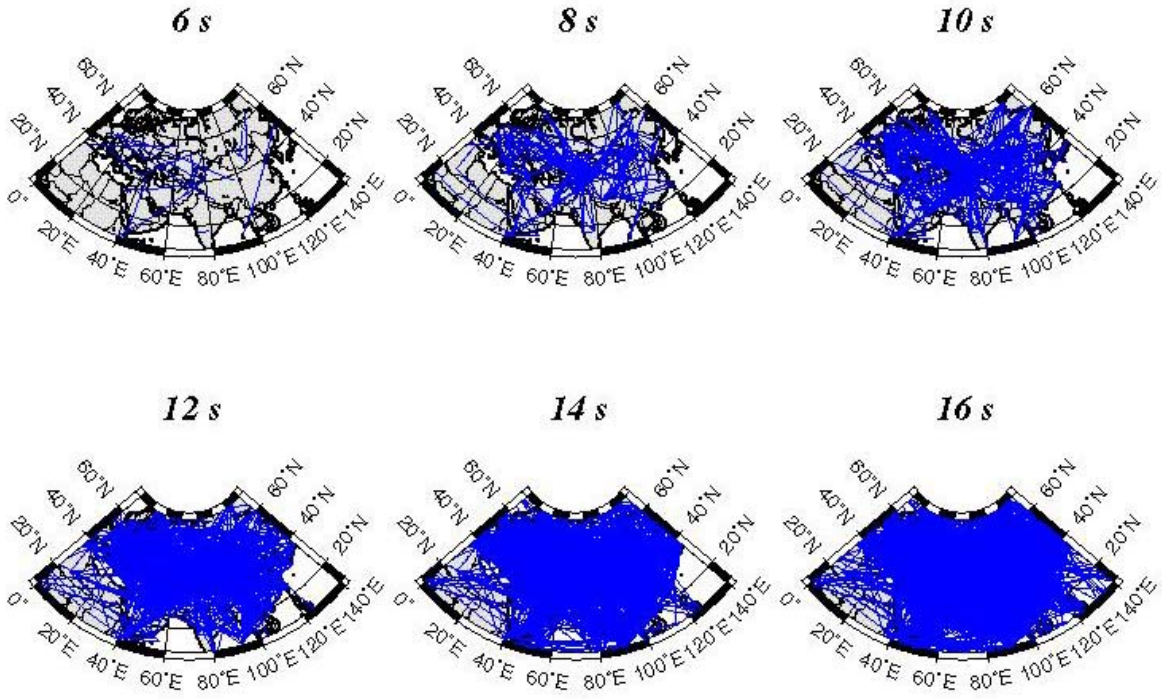

Figure 4. Paths for which the spectral amplitudes were measured at indicated periods.

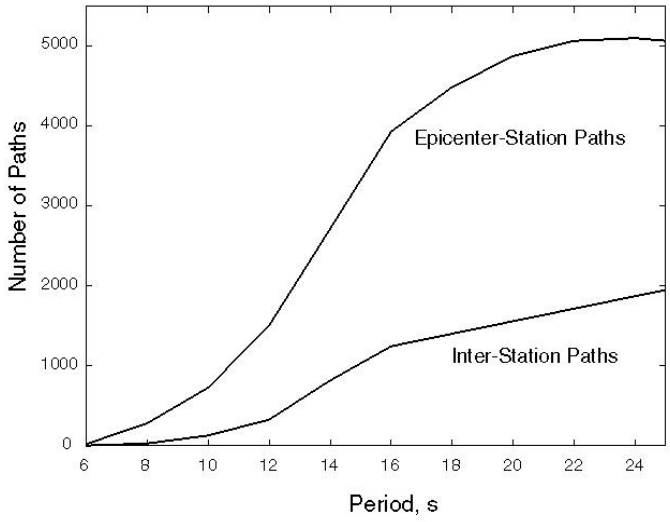

Figure 5. Numbers of selected epicenter/station paths and interstation paths as functions of periods.

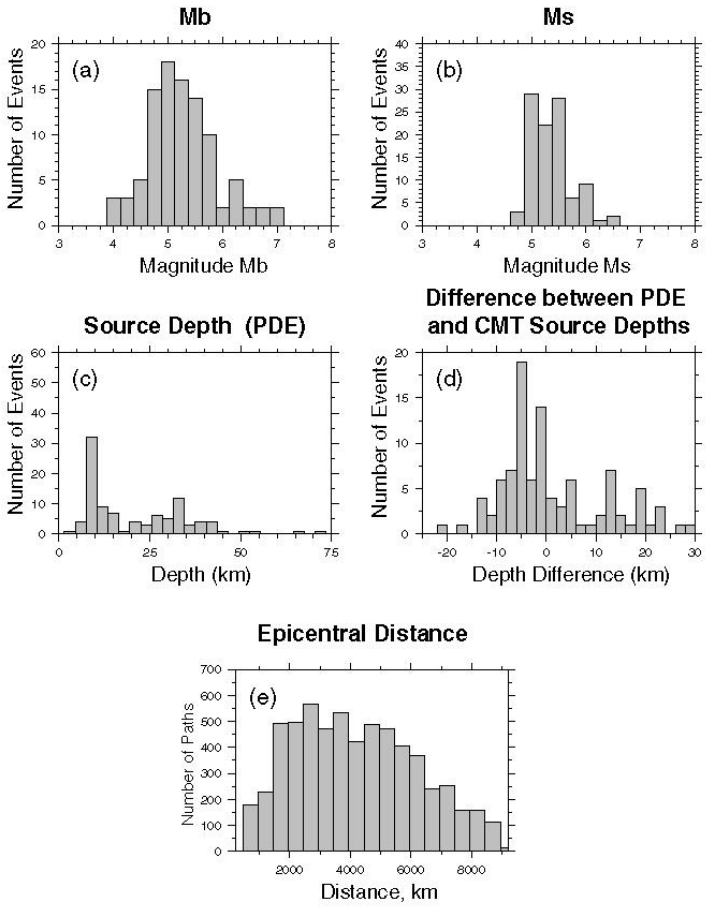

Figure 6. Histograms characterizing the events and paths in the data set.

Figure 7 demonstrates the repeatability of measurements for the set of closely spaced events (doublets) in Turkey. The almost-identical events should generate quite similar amplitude spectra. However, an ~10% difference in amplitudes is observed at short periods, even after the normalization by the slightly different seismic moments, Mo. This may be caused by slight differences in source depths not reflected in the PDE catalog.

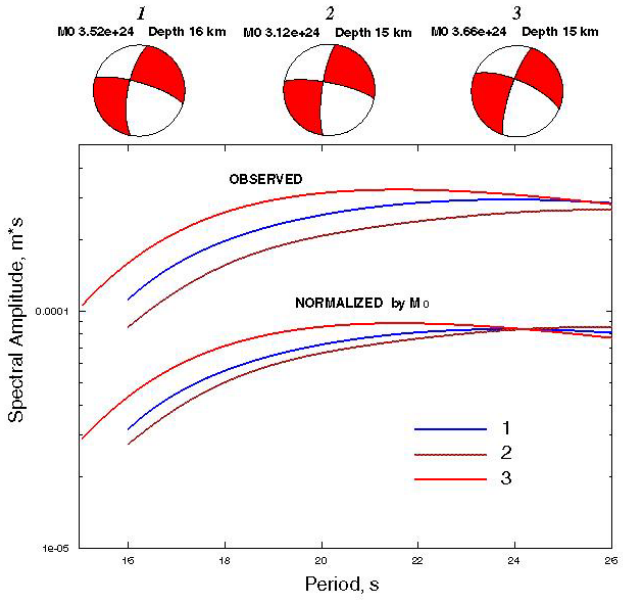

Figure 7. Similarity of amplitude spectra for three close local events in Turkey.

The effect of uncertainties in source parameters may be mitigated by using the interstation measurements. We select for such measurements the stations that are at nearly the same azimuth from the epicenter (with a difference of less than 1 degree). The number of such measurements as a function of period is presented in Figure 5. Figure 8 shows two examples of interstation combinations. In the left panel, spectra observed from three stations in the KNET network are compared with the spectrum observed at station ARU, about ~2000 km from KNET. The close similarity of spectra observed at different KNET stations and their compatibility with the spectrum observed at ARU are evident. In the right panel of Figure 8, the compatibility of spectra obtained by station USP (KNET) and KURK (KAZNET) is similarly demonstrated.

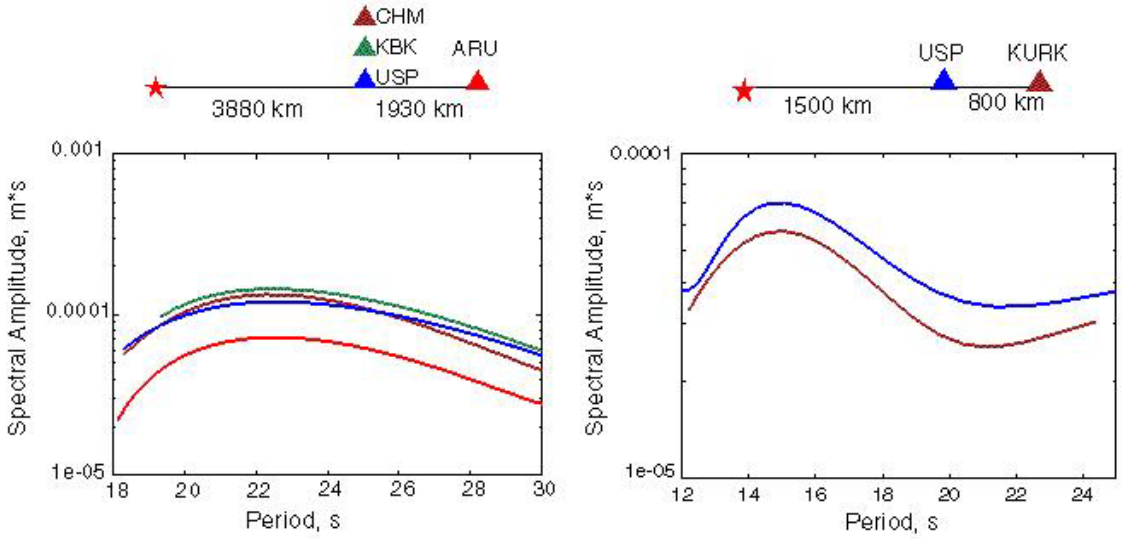

Figure 8. Examples of interstation measurements by stations of KAZNET and KNET networks: event near Andaman Islands (left); event in Pakistan (right).

Interpreting Amplitude Spectra Measurements

The transition from amplitude spectra to attenuation coefficients for the source to receiver paths is based on information about the source mechanism and depth, which is usually taken from the Harvard-CMT catalog. Uncertainties in CMT solutions for the best double couple orientation and source depth have a strong influence on the attenuation coefficients. We illustrate this by simulating the effects of uncertainties in source mechanism, when strike, dip, and slip determining the best couple are varied by ±5 degrees (Figure 9, left). The simulation is performed for a realistic crustal model and source parameters. Variations in the amplitude spectrum are on the order of 10%. More dramatic effects are produced by the uncertainty in the source depth (Figure 9, right). The maximum uncertainty in the spectrum occurs where the source excitation function experiences a minimum near the source depth. Although the details will depend on source mechanism and local structure, this simulation shows that a 5 km error in source depth (see Figure 5d, comparing depth estimates from different catalogs) may produce up to a 50% error in the spectral measurements at periods between 10 s and 20 s. If the event depth is known to lie between 15 and 25 km, the amplitude spectra are expected to be similar between 10 and 20 s. Spectra in this period range are very sensitive to the depth of shallower events. Interstation measurements are significantly less sensitive to these factors, but the number of these measurements is much lower than for source/receiver measurements (Figure 5).

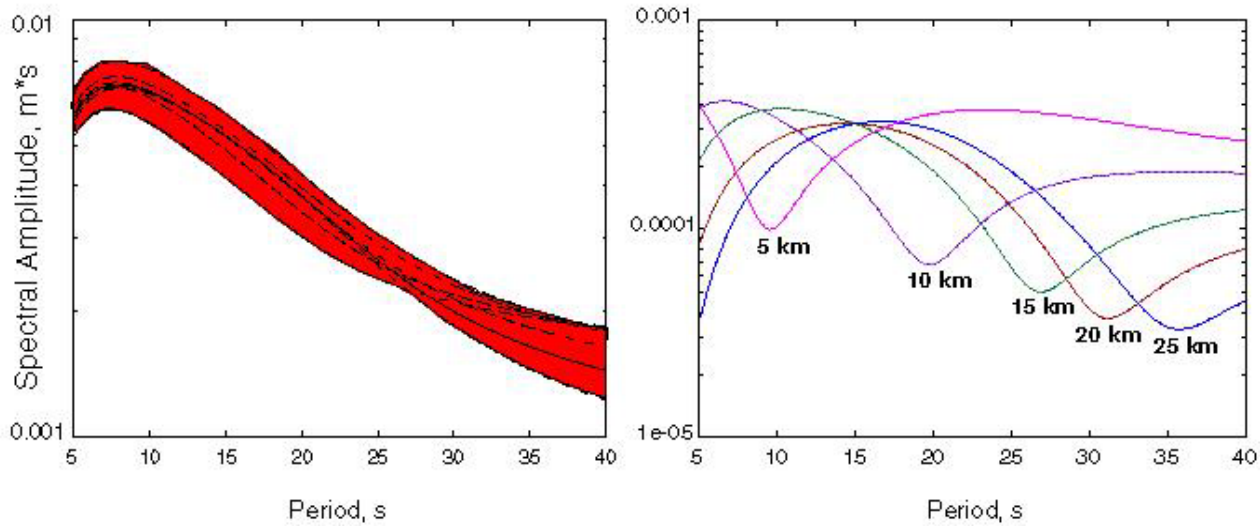

Figure 9. Effects of uncertainties in source parameters. The red stripe (left) corresponds to the possible range of spectral amplitudes when strike, dip, and slip, determining the best couple, vary by±5%. The source depth (right) varies from 5 to 30 km.

Effects of Lateral Inhomogeneities

Uncertainties in the 3-D structure of the crust may also distort the estimated attenuation coefficients. This may happen because of significant differences in the crustal structure near the source and receiver locations (single-station case) or near the location of the receivers (interstation case).

Shown in Figure 10 is a simulated example is shown in Figure 10 for dramatically different crustal structures at source and receiver. This effect is not as severe as the effect of uncertainty in source depth. In addition, its effect can be ameliorated in the transition from amplitude spectra to attenuation coefficients by using an existing 3-D model of the Eurasian crust (e.g., Shapiro and Ritzwoller, 2002).

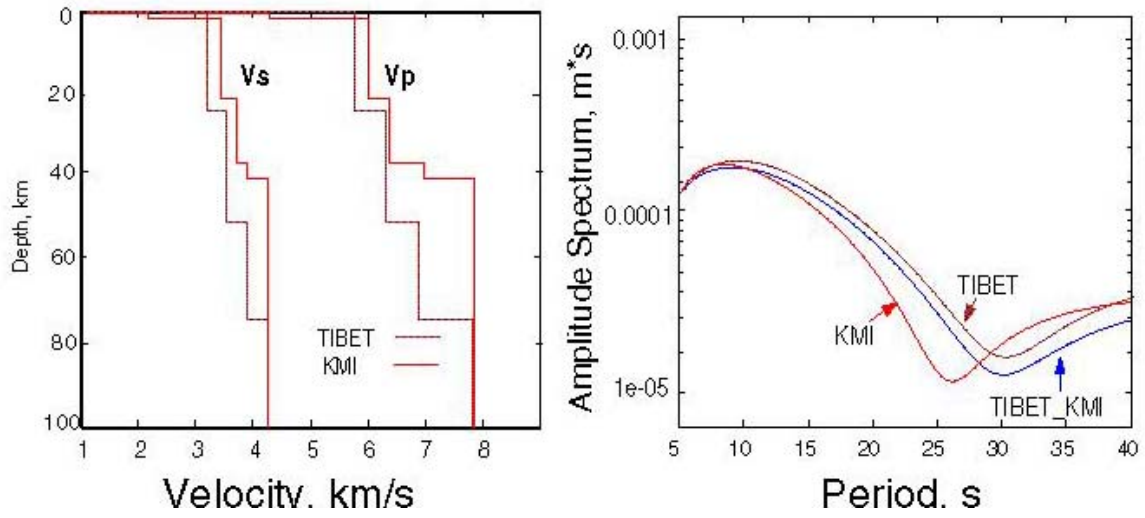

Figure 10. The differences in synthetic amplitude spectra for the path from Tibet to station KMI and a realistic source mechanism. Crustal models under the source (TIBET) and receiver (KMI) are shown on the left. Synthetic amplitude spectra for three different simulations appear on the right. The TIBET curve is for the TIBET model at both event and station locations; the KMI curve is for the KMI model at both location. The TIBET-KMI curve is for the TIBET model near the source and KMI model under the station.

CONCLUSIONS AND RECOMMENDATIONS

We described here the first stage of the study dedicated to the construction of the attenuation model for short-period waves across Central Asia. Only three years (2003-2005) of data have been used up to now.

The modified SWAMTOOL technique permits reliable measurement of surface-wave amplitude spectra and evaluation of the quality of measurements. We found that the existing networks and the pattern of seismicity will provide a significant amount of data on spectral amplitudes for periods in the range 12-20 s, appropriate for 2-D tomographic inversion for attenuation coefficients. Data for shorter periods are too scarce for tomographic inversion.

The synthetic examples demonstrate the strong dependence of the Rayleigh-wave amplitude spectra on source parameters, particularly the source depth and the structure of the crust at source and receiver regions. This implies the necessity to include some additional unknowns related to the source into the inversion of observed data and to use an existing 3-D model of the Eurasian crust in the data-inversion process. Inclusion of additional unknowns such as a source depth, seismic moment, and angles determining source geometry will address some of the uncertainties discussed in this report.

We plan to continue data acquisition and processing as well as developing the robust algorithm for data inversion, taking into account uncertainties in source parameters and the 3-D structure of the Eurasian crust.

ACKNOWLEDGEMENTS

The authors highly appreciate the opportunity to receive digital records from IRIS DMC, GEOSCOPE, and GEOFON.

REFERENCES

Bonner, J. L., D. R. Russel, D. G. Harkrider, D. T. Reiter, and R. B. Herrmann (2006). Development of a time-domain, variable-period surface wave magnitude measurement procedure for application at regional and teleseismic distances, *Bull. Seism. Soc. Am*. 96: 678-696.

Herrin, E. E. and T. T. Goforth (1977). Phase-matched filters: Application to the study of Rayleigh waves, *Bull. Seism. Soc. Am*. 67: 1259-1275.

Levshin, A. L., T. B. Yanovskaya, A. V. Lander, B. G. Bukchin, M. P. Barmin, L. I. Ratnikova, and E. N Its (1989). *Seismic Surface Waves in Laterally Inhomogeneous Earth*. (Ed. V.I. Keilis-Borok), Kluwer Publ. House.

Levshin, A. L. and M. H. Ritzwoller (2003). Discrimination, Detection, Depth, Location, and Wave Propagation Studies Using Intermediate Period Surface Waves in the Middle East, Central Asia, and the Far East, Technical Report DTRA-TR-01-28, Defense Threat Reduction Agency, 120 pp.

Levshin, A. L., J. L. Stevens, M. H. Ritzwoller, D. A. Adams, and G. E. Baker (2003). Improvement of Detection and Discrimination Using Short Period (7s-15s) Surface Waves in W. China, N. India, Pakistan and Environs, Final Report*,* submitted to Defense Threat Reduction Agency, 49 pp.

Marshall, P. D. and P. W. Basham (1972). Discrimination between earthquakes and underground explosions employing an improved Ms scale, *Geophys. J. R. Astr. Soc*. 28: 431-458.

Mitchell, B. J. (1995). Anelastic structure and evolution of the continental crust and upper mantle from seismic surface wave attenuation, *Rev. Geophys*. 33: 441-462.

Ritzwoller, M. H. and A. L. Levshin (1998). Eurasian surface wave tomography: Group velocities*, J. Geophys. Res.* 103: 4839-4878.

Russell, D. R., R. B. Herrman, and H. Hwang (1988). Application of frequency-variable filters to surface wave amplitude analysis, *Bull. Seism. Soc. Am*. 78: 339-354.

Russell, D. R. (2006). Development of a time-domain, variable-period surface wave magnitude measurement procedure for application at regional and teleseismic distances, Part I: Theory, *Bull. Seism. Soc. Am*. 96: 665-677.

Selby, N. D. and J. H. Woodhouse (2000). Controls on Rayleigh wave amplitudes: Attenuation and focusing, *Geophys. J. Int.* 142: 933-940.

Shapiro, N. M. and M. H. Ritzwoller (2002). Monte-Carlo inversion for a global shear-velocity m\model of the crust and upper mantle, *Geophys. J. Int*. 151: 88-105.

Stevens, J. L., D. A. Adams, and G. E. Baker (2001). Improved surface wave detection and measurement using phase-matched filtering with a global one-degree dispersion model, in *Proceedings of the 23rd Seismic Research Review: Worldwide Monitoring of Nuclear Explosions,* LA-UR-01-4454, Vol. 1, 420-430.

Woodhouse, J. H. (1974). Surface waves in a laterally varying layered structure, *Geophys. J. Roy. Astr. Soc*. 37: 461-490.

Yang, X., S. R. Taylor, and H. J. Patton (2004). The 20-s Rayleigh wave attenuation tomography for central and southeastern Asia, *J. Geophys. Res.* 108, B12304, doi:10.1029/2004JB003193.

Yang, X, A. R. Lowry, A. L. Levshin, and M. H. Ritzwoller (2005). Toward a Rayleigh wave attenuation model for Eurasia and calibrating a new M_S formula, in *Proceedings of the 27th Seismic Research Review, Ground-Based Nuclear Explosion Monitoring Technologies,* LA-UR-05-6407*,* 259-265.